

# Measuring the effects of rheology and regional tectonics on the syntectonic rocks of a migmatitic complex from Cap de Creus

## *Efectos de la reología y de la tectónica regional en las rocas sintectónicas del complejo migmatítico de Cap de Creus*

David Candami<sup>1</sup>, Elena Druguet<sup>1</sup> and Pere Enrique<sup>2</sup>

<sup>1</sup> Departament de Geologia, Universitat Autònoma de Barcelona, 08193-Bellaterra, Barcelona, España.

dcandami@gmail.com elena.druguet@uab.cat

<sup>2</sup> Departament de Geoquímica, Petrologia i Prospecció Geològica, Universitat de Barcelona, Martí Franquès s/n. 08028-Barcelona, España.

pere.enrique@ub.edu

### ABSTRACT

To deepen the understanding of the interactions between tectonics and magmatism in the mid to deep crust, a detailed petrostructural analysis has been performed in the southern area of Punta dels Farallons-Volt Andrau (Cap de Creus, Eastern Pyrenees). In this area, schists under high-grade conditions suffered partial melting while a sequence of intermediate to acid magmatic rocks were emplaced during the Variscan D2 transpressive deformation event. Both regional tectonics and rheological features controlled the way deformation localized in the various rocks of the migmatitic complex. Schists and migmatites have a penetrative sub-vertical foliation (S2). Strain measurements of deformed late veins and dykes have allowed us to determine the regional deformation post-dating their emplacement. Dextral transpression was associated to N-S sub-horizontal shortening and the principal extension direction switched from sub-vertical to sub-horizontal under bulk constriction to plane strain.

**Key-words:** Anatexis, Cap de Creus, deformation, granitoid, migmatite.

### RESUMEN

A fin de profundizar en la comprensión de las interacciones entre tectónica y magmatismo en la corteza media y profunda, se ha realizado un análisis petroestructural detallado en el sector meridional de Punta dels Farallons-Volt Andrau (Cap de Creus, Pirineos Orientales). En esta zona, esquistos de alto grado fueron afectados por fusión parcial e intruídos por una secuencia de rocas magmáticas intermedias a ácidas durante la fase deformativa transpresiva varisca (D2). Tanto la tectónica regional como las características reológicas controlaron el modo de localización de la deformación en las distintas rocas del complejo migmatítico. Los esquistos y migmatitas presentan una marcada foliación sub-vertical (S2). Las medidas de deformación de venas y diques tardíos han permitido determinar la deformación regional post-emplazamiento. La transpresión dextral fue asociada a un acortamiento sub-horizontal N-S y la dirección de extensión principal pasó de sub-vertical a sub-horizontal bajo un régimen constriccional muy próximo a "plane strain".

**Palabras clave:** Anatexia, Cap de Creus, deformación, granitoides, migmatita.

Geogaceta, 54 (2013), 91-94.  
ISSN (versión impresa): 0213-683X  
ISSN (Internet): 2173-6545

Fecha de recepción: 31 de enero de 2013  
Fecha de revisión: 25 de abril de 2013  
Fecha de aceptación: 24 de mayo de 2013

## Introduction

Regional deformation during partial melting and magmatism has a major effect on the resulting rock structures (Sawyer, 2008). Moreover, the structural features of migmatitic terranes are also influenced by rheological parameters (Vanderhaeghe, 2009).

The Punta dels Farallons-Volt Andrau area is one of the migmatitic complexes in the Variscan basement of the north Cap de Creus (Fig. 1). The area consists of partially migmatized sillimanite schists, small heterogeneous bodies of quartz gabbro, quartz

diorite and granitoids, and a widespread network of pegmatite dykes (Druguet, *et al.*, 1995). The magmatic rocks are grouped in two associations: a calc-alkaline association that includes quartz gabbro, quartz diorite, tonalite, granodiorite and granite, and a peraluminous association represented by leucogranites and pegmatites. This later association is likely derived from partial melting of the pelitic peraluminous host schists (Damm *et al.*, 1992; Druguet, *et al.*, 1995), although an origin by fractionation of a granitoid magma is postulated by other authors (Alfonso and Melgarejo, 2003).

Druguet and Hutton (1998) showed

that local anatexis and magmatism (from basic, to intermediate and acidic) in the Cap de Creus migmatitic complexes took place under the Variscan D<sub>2</sub> regional dextral transpression.

This paper analyzes the structural features of different lithologies around a transitional domain between high-grade sillimanite schists and migmatitic and magmatic rocks at the southern area of the Punta dels Farallons-Volt Andrau migmatitic complex. It is aimed to determine the rheological behavior of different materials, to estimate regional deformation and kinematics from deformed veins and dykes, and to

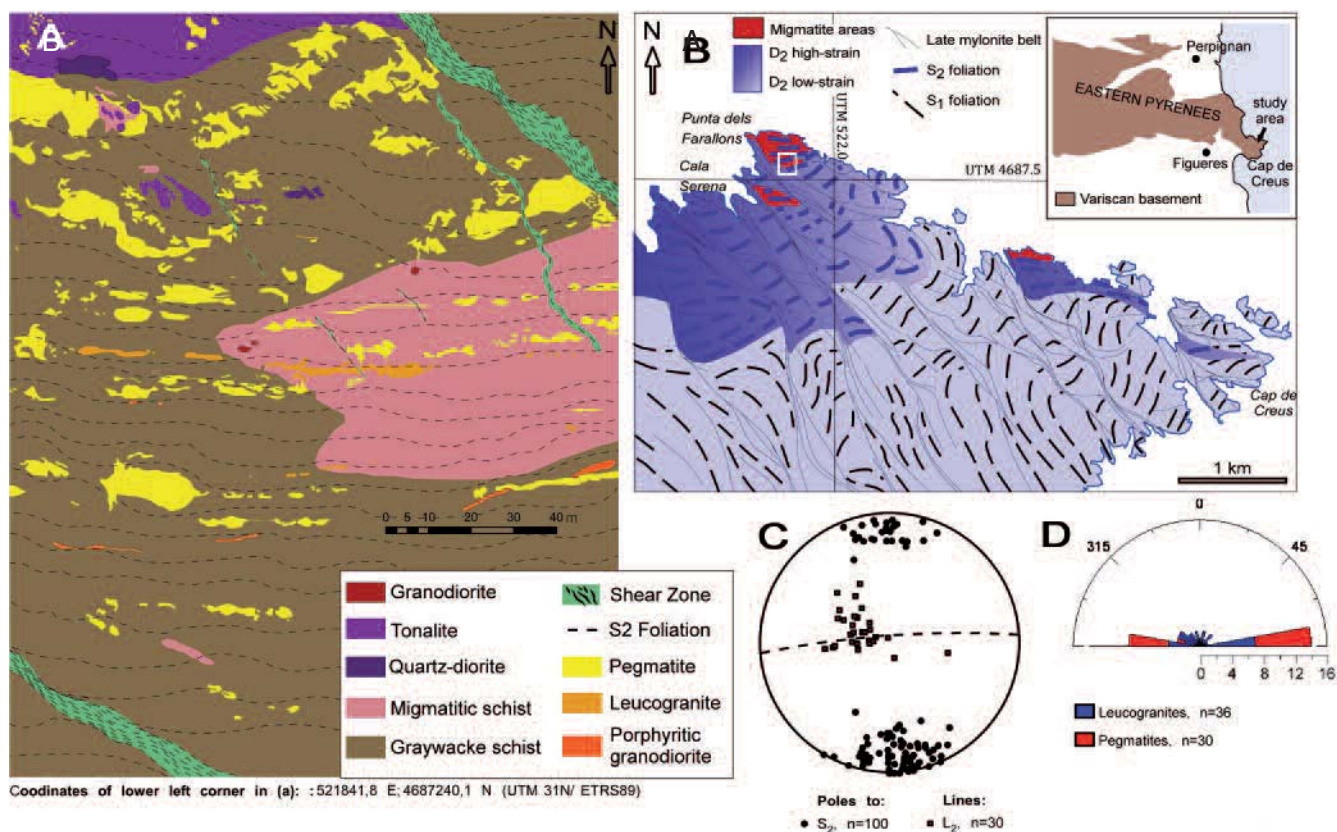


Fig. 1.- A) Geological setting of the study area in the northern Cap de Creus. B) Lithological and structural map of the study area at south Volt Andrau. C) Stereographic projection of poles to  $S_2$ , mean plane and stretching lineation ( $L_2$ ). D) Rose diagram of orientation frequency of the leucogranite and pegmatite veins and dykes that are folded or boudinaged.

Fig. 1.- A) Situación geológica del área de estudio en la región septentrional del Cap de Creus. B) Mapa de litologías y estructuras en el área de estudio al sur de Volt Andrau. C) Proyección estereográfica de los polos de  $S_2$ , plano promedio de la  $S_2$  y línea de estiramiento ( $L_2$ ). D) Diagrama de rosas de frecuencia de orientación de los diques y venas de leucogranito y pegmatita plegados o boudinados.

establish a petrostructural model for the evolution of the migmatitic complex.

### Petrostructure of South Volt Andrau

The area is characterized by the presence of two types of high-grade schists. The most abundant type consists of mm-banded greywacke schists with quartz-feldspathic zones and darker zones rich in  $Bt \pm Crd \pm Sil$ . This layering has a sub-parallel foliation ( $S_1$ ) both being both folded by the  $D_2$  deformation phase (Fig. 2D). Fold axes are subvertical and parallel to  $L_2$  stretching lineation (Fig. 1C).

The migmatitic schists, which are predominant in the northeastern area, are stromatic and composed by coarse grained quartz-feldspathic bands (leucosome) of mm- to cm-thickness surrounded by mafic bands (melanosome), and bands of greywacke schists (mesosome). The relative percentages of leucosome, melanosome and mesosome vary around 30%, 15% and

55% respectively (Fig. 2A). This fact allows classifying these migmatites as metatexites (Sawyer, 2008). The stromatic banding is parallel to the regional E-W  $S_2$  foliation (Fig. 1). These migmatitic schists are interpreted as derived from partial melting of metapelites during  $D_2$ .

The igneous rocks are heterogeneously distributed, although specially localized in the north (Fig. 1B). In this area, quartz diorites and tonalites predominate and form irregular elongated bodies in a E-W direction. They show a weak sub-vertical gneissic foliation that correlates with the  $S_2$  in the schists. These bodies are crosscut by all the others intrusive rocks. Granodiorite bodies have irregular to sub-tabular shapes and can be folded with the metamorphic host rocks, while they present a gneissic foliation parallel to the fold axial planes and the  $S_2$  in the schists, proving the syntectonic character of these rocks with  $D_2$  (Fig. 2B). The porphyritic granodiorite constitutes a  $S_2$ -parallel E-W trending dyke of 2 m thickness. An E-W gneissic foliation overprints the por-

phyritic texture (Fig. 2C). The elliptical enclaves present in this dyke have a sub-vertical major axis that correlates with  $L_2$  in the schists.

The latest intrusions are leucogranites and pegmatites, which are present all over the study area. Leucogranites form a swarm composed by veins and dykes of variable dimensions, with lengths between a few cm and 20 m and thickness from a few mm up to 3 m, while pegmatites generally form larger bodies or dykes. According to their orientation (Fig. 1D), both leucogranites and pegmatites can be ptymatically folded or boudinaged (Fig. 2D, E) and are generally devoid of internal planar fabric. The pegmatites have a predominantly E-W direction and cut all the previously described structures.

### Rheological aspects

As described in the previous section, the diverse lithologies show different styles and degrees of deformation according to

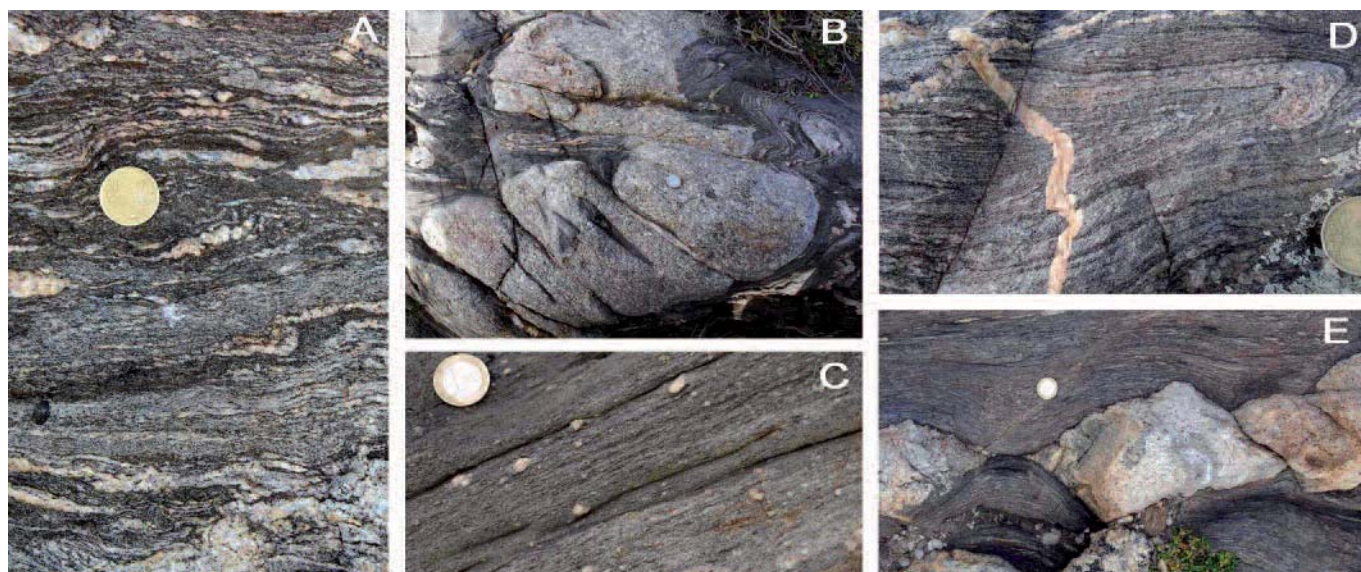


Fig. 2.- Field photographs from the study area in South Volt Andrau. A) Stromatic migmatite with differentiated leucosome, melanosome and mesosome layers. Layering is parallel to  $S_2$  foliation. B) Folded sub-tabular granodiorite body showing an internal axial planar  $S_2$  foliation. C) Detail of  $S_2$  gneissic foliation in a porphyritic granodiorite. Feldspar phenocrysts are surrounded by the deformed matrix. D) A  $D_2$  syntectonic leucogranite vein cross-cuts the folded schists. Both are coplanarly folded with a marked difference in strain: tight folds in the schists and open folds in the vein. E) Asymmetrically boudinaged leucogranite dyke. Boudins are delimited by dextral shear fractures.

Fig. 2.- Fotografías de campo de la zona de estudio al sur de Volt Andrau. A) Bandas de leucosoma, melanosoma y mesosoma en una migmatita estromática. El bandeo es paralelo a la foliación  $S_2$ . B) Cuerpo granodiorítico sub-tabular plegado y mostrando una foliación  $S_2$  de plano axial. C) Detalle de la foliación gnéissica  $S_2$  desarrollada en una granodiorita porfídica. D) Vena leucogranítica sintectónica cortando esquistos plegados. Nótese el plegamiento coplanar de ambos pero con marcada diferencia en el grado de deformación: pliegues apretados en los esquistos y abiertos en la vena. E) Dique leucogranítico con boudinage asimétrico. Los boudins están limitados por fracturas de cizalla dextral.

their original shapes, orientations and times of emplacement with regard to  $D_2$ . In addition, it is envisaged that deformation also depends on rheological aspects, particularly on the competence contrast between different lithologies, which mainly depends on their mineralogical compositions and textural properties.

Meso- and micro-scale structures provide a qualitative indication about these rheological contrasts. Thus, different rock types can be ordered in an increasing degree of relative competence as: (1) migmatitic schists (melanosome and mesosome) and metagreywackes as the more incompetent rocks, (2) quartz-diorites and granitoids, (3) leucogranites and (4) pegmatites as the more competent rocks.

For a more accurate estimation of competence contrast ( $m$ ) we have applied the technique of Schmalholz and Podladchikov (2001) estimating strain and competence contrast for the leucogranitic veins emplaced in various country-rocks. This is obtained from the relations between fold amplitude ( $A$ ), fold wavelength ( $\lambda$ ) and thickness ( $H$ ) and plotting them on a strain contour map (Fig. 3). The highest competence contrasts (average  $m \approx 50$ ) are observed in leucocratic veins (leucosomes and leucogranites) emplaced

in schists, with a maximum value of  $m = 150$ . The competence contrast decreases for the leucogranitic veins emplaced in (or cutting) the granodioritic host rock ( $m \approx 25$ ), and is even smaller in a tonalitic host rock ( $m \approx 10$ ). These results are consistent with the presence of pygmatic folds and boudins in veins emplaced into schists, a fact that contrasts with the scarcity of folds and, instead, the pres-

ence of a weak internal planar fabric in those veins which are intruded into granitoids or quartz-diorites. The shortening values obtained by this method vary between 20% and 55%.

### Estimation of post-dyke strain

Because of the high competence contrast between leucogranites and schists,

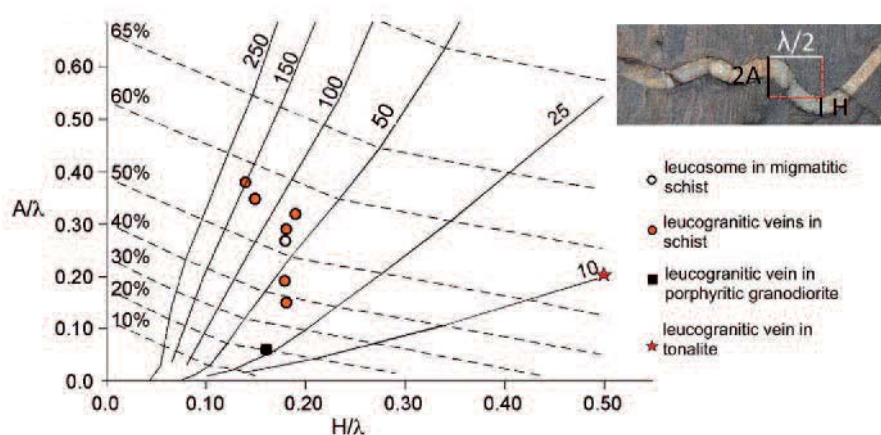


Fig. 3.- Ratios of  $A/\lambda$  and  $H/\lambda$  from measured fold profiles in leucocratic veins plotted in the strain contour map of Schmalholz and Podladchikov (2001). The solid lines refer to the competence contrasts and the dashed lines to the percentage of vein shortening.

Fig. 3 Relaciones  $A/\lambda$  y  $H/\lambda$  a partir de medidas de perfiles de pliegues en venas leucocráticas, representadas en el mapa de contornos de deformación de Schmalholz y Podladchikov (2001). Las líneas continuas hacen referencia a los contrastes de competencia ( $m$ ) y las discontinuas, al porcentaje de acortamiento de las venas.

leucogranites become suitable as strain markers. Thus, a semi-quantitative strain analysis was performed from 22 stretched (folded and boudinaged) veins on sub-horizontal outcrops to determine the  $D_2$  post-dyke strain ellipse, based on the method by De Paor (1988). From this 2D analysis, a 3D strain ellipsoid was then determined by assuming constant volume deformation ( $X \times Y \times Z = 1$ ), which is reasonable for mid to deep crustal levels. The results are depicted in figure 4. It should be noticed that the obtained 25%  $D_2$  regional shortening and bulk axial ratio  $R_{xz} = 1.83$  post-dating the dykes represent minimum values of strain, since the method assumes that the veins or dykes have not any homogeneous deformation.

### Model of emplacement and deformation

The performed field analysis allows us presenting a model of the petrostructural evolution of the migmatitic complex in four main stages (Fig. 4).

1. Intrusion of quartz diorite and tonalite bodies induced partial melting of pelitic schists in a  $D_2$  dextral transpressive regime involving sub-vertical extension (see Fig. 1C).

2. Sub-tabular bodies of granodiorite were emplaced during progressive  $D_2$  deformation.

3. Leucocratic magmas (leucogranitic and pegmatitic veins and dykes) represent the latest intrusions. They were emplaced either into NW-SE trending extension fractures, or following the E-W oriented  $S_2$  foliation.

4.  $D_2$  deformation post-dating the emplacement of leucogranites and pegmatites was characterized by progressive transpression with the main extension direction switching from sub-vertical to sub-horizontal, as indicated by the performed strain analysis. Dykes and veins of high competence were folded or boudinaged depending on their initial orientation. Post-dyking shortening associated to regional transpression was >25%, with a N-S trending main shortening direction.

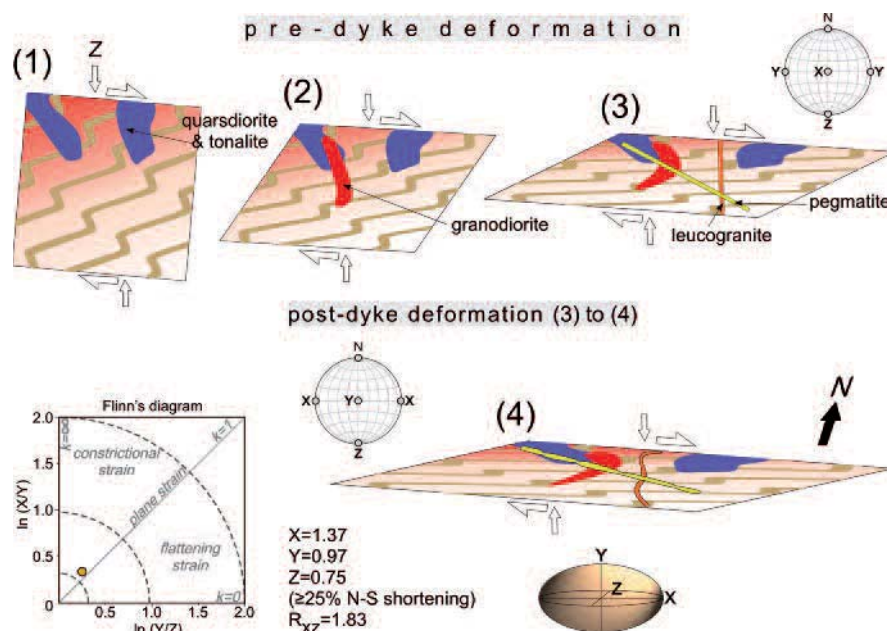


Fig. 4.- Four-stages model of the petrostructural evolution of the South Volt Andrau migmatite area, depicted in diagrams, stereonets, strain ellipsoid and Flinn (1962) diagram. X, Y, Z are the maximum, intermediate and minimum strain axes respectively and  $R_{xz}$  is the axial ratio of the bulk strain in the sub-horizontal section. See the main text for further explanation.

Fig. 4.- Modelo en cuatro estadios de evolución petroestructural del área migmatítica al sur de Volt Andrau, representado en diagramas, estereogramas, elipsoide de deformación y diagrama de Flinn (1962). X, Y y Z son los ejes máximo, intermedio y mínimo de deformación respectivamente, y  $R_{xz}$  la relación axial de deformación global en el plano sub-horizontal. Ver explicaciones en el texto principal.

### Conclusions

The field observations and structural analyses in a domain of the Punta dels Farallons-Volt Andrau migmatitic complex (Cap de Creus) corroborate the syntectonic emplacement of a sequence of intermediate to acid magmatic rocks during the Variscan dextral transpressive deformation event ( $D_2$ ).

The performed measurements of deformed late leucocratic veins and dykes have allowed us to determine the regional strain and kinematics post-dating their emplacement. Dextral transpression was associated to sub-horizontal regional shortening >25%, with the principle extension direction switching from sub-vertical to sub-horizontal under bulk constrictional to plane strain conditions.

This study also emphasizes the role of rheological contrasts in the structural evolution of complexly deformed migmatitic terranes.

### Acknowledgments

This work was partly funded by the Spanish MICINN project CGL2010–21751.

### References

- Alfonso, P., Melgarejo, J.C., Yusta, I. and Velasco, F. (2003). *The Canadian Mineralogist* 41, 103–116.
- Damm, K.W., Harmon, R.S., Heppner, P.M. and Dornsiepen, U. (1992). *Geological Journal* 27, 76–86.
- De Paor, D.G. (1988). *Journal of Structural Geology* 10, 639–642.
- Druguet, E. and Hutton, D.H.W. (1998). *Journal of Structural Geology* 20, 905–916.
- Druguet, E., Enrique, P. and Galán, G. (1995). *Geogaceta* 18, 199–202.
- Flinn, D. (1962). *Quarterly Journal of the Geological Society* 118, 385–428.
- Sawyer, E.W. (2008). *Atlas of migmatites*. NRC Research Press, Canada, 371 p.
- Schmalholz, S.M. and Podladchikov, Y.Y. (2001). *Tectonophysics* 340, 195–213.
- Vanderhaeghe, O. (2009). *Tectonophysics* 477, 119–134.